Novel Non-Heteroarylpyrimidine (HAP) capsid assembly modifiers have a different mode of action from HAPs *in vitro*

Angelica Corcuera[a,b], Katharina Stolle[a], Stefan Hillmer[c], Stefan Seitz[b], Ji-Young Lee[b], Ralf Bartenschlager[b,d], Alexander Birkmann[a], and Andreas Urban[a*]

[a]AiCuris Anti-infective Cures GmbH, Friedrich-Ebert-Str.475, 42117 Wuppertal, Germany

[b]Department of Infectious Diseases, Molecular Virology, Heidelberg University, Im Neuenheimer Feld 344, 69120 Heidelberg, Germany

[c]Electron Microscopy Core Facility, Heidelberg University, Im Neuenheimer Feld 345, 69120 Heidelberg, Germany

[d]German Center for Infection Research, Heidelberg Partner Site, Im Neuenheimer Feld 344, 69120 Heidelberg, Germany

*Corresponding author: andreas.urban@aicuris.com

https://doi.org/10.1016/j.antiviral.2018.07.011

© 2018. This manuscript version is made available under the Creative Commons Attribution License (CC BY 4.0) https://creativecommons.org/licenses/by/4.0/.

Antiviral Research 158 (2018) 135–142

Contents lists available at ScienceDirect

Antiviral Research

journal homepage: www.elsevier.com/locate/antiviral

Novel non-heteroarylpyrimidine (HAP) capsid assembly modifiers have a different mode of action from HAPs *in vitro*

Angelica Corcuera[a,b], Katharina Stolle[a], Stefan Hillmer[c], Stefan Seitz[b], Ji-Young Lee[b], Ralf Bartenschlager[b,d], Alexander Birkmann[a], Andreas Urban[a,*]

[a] AiCuris Anti-infective Cures GmbH, Friedrich-Ebert-Str.475, 42117, Wuppertal, Germany
[b] Department of Infectious Diseases, Molecular Virology, Heidelberg University, Im Neuenheimer Feld 344, 69120, Heidelberg, Germany
[c] Electron Microscopy Core Facility, Heidelberg University, Im Neuenheimer Feld 345, 69120, Heidelberg, Germany
[d] German Center for Infection Research, Heidelberg Partner Site, Im Neuenheimer Feld 344, 69120, Heidelberg, Germany

ARTICLE INFO

Keywords:
HBV
Core protein
Capsid
Capsid assembly modifier
Heteroarylpyrimidine

ABSTRACT

One of the most promising viral targets in current hepatitis B virus (HBV) drug development is the core protein due to its multiple roles in the viral life cycle. Here we investigated the differences in the mode of action and antiviral activity of representatives of six different capsid assembly modifier (CAM) scaffolds: three from the well-characterized scaffolds heteroarylpyrimidine (HAP), sulfamoylbenzamide (SBA), and phenylpropenamide (PPA), and three from novel scaffolds glyoxamide-pyrrolamide (GPA), pyrazolyl-thiazole (PT), and dibenzothiazepin-2-one (DBT). The target activity and antiviral efficacy of the different CAMs were tested in biochemical and cellular assays. Analytical size exclusion chromatography and transmission electron microscopy showed that only the HAP compound induced formation of aberrant non-capsid structures (class II mode of action), while the remaining CAMs did not affect capsid gross morphology (class I mode of action). Intracellular lysates from the HepAD38 cell line, inducibly replicating HBV, showed no reduction in the quantities of intracellular core protein or capsid after treatment with SBA, PPA, GPA, PT, or DBT compounds; however HAP-treatment led to a profound decrease in both. Additionally, immunofluorescence staining of compound-treated HepAD38 cells showed that all non-HAP CAMs led to a shift in the equilibrium of HBV core antigen (HBcAg) towards complete cytoplasmic staining, while the HAP induced accumulation of HBcAg aggregates in the nucleus. Our study demonstrates that the novel scaffolds GPA, PT, and DBT exhibit class I modes of action, alike SBA and PPA, whereas HAP remains the only scaffold belonging to class II inhibitors.

1. Introduction

Although an effective prophylactic vaccine against hepatitis B virus (HBV) infection is available since the 1980s, around 257 million people still suffer from chronic HBV infection worldwide. In 2015, an estimated loss of 32 million disability-adjusted life years and 887,000 deaths was attributed to HBV infection, most notably due to the resulting liver cirrhosis and hepatocellular carcinoma (World Health Organization, 2017). Current treatments reduce viral load either by inhibition of the viral reverse transcriptase via nucleoside/nucleotide analogs or immunomodulation induced by pegylated interferon-alpha. However, as these treatments do not cure the infection, patients require long-term or lifelong therapy. Consequently, the major goal of current anti-HBV drug discovery is to develop novel drugs with new modes of action resulting in virus elimination or at the least a functional HBV cure, i.e. sustained, undetectable hepatitis B surface antigen (HBsAg) and HBV DNA in the serum with or without anti-HBs seroconversion (Lok et al., 2017).

HBV is a small enveloped DNA virus with a 3.2 kB, partially double-stranded, relaxed circular DNA (rcDNA) genome (Kay and Zoulim, 2007). Its chromatin-like viral minichromosome persists in the nucleus of infected cells in the form of a covalently closed circular DNA (cccDNA). Of the various potential drug targets including the 7 viral proteins, cccDNA, and HBV entry itself, the core protein (Cp) is one of the most promising targets.

The Cp (21 kDa) has two domains: an alpha-helix rich N-terminal assembly domain composed of residues 1–149 (Cp149, ~17 kDa), and an arginine-rich C-terminal domain (CTD, ~4 kDa) composed of the remaining 34–36 residues (depending on the genotype). The Cp forms homodimers with an interface composed of four helices, two from each

* Corresponding author.
E-mail address: andreas.urban@aicuris.com (A. Urban).

https://doi.org/10.1016/j.antiviral.2018.07.011
Received 25 May 2018; Received in revised form 12 July 2018; Accepted 17 July 2018
Available online 20 July 2018
0166-3542/ © 2018 Elsevier B.V. All rights reserved.

List of abbreviations

aSEC	analytical size exclusion chromatography
AUC	area under the curve
CAA	biochemical capsid assembly assay
CAM	capsid assembly modifier
CC_{50}	half maximal cytotoxic concentration
cccDNA	covalently closed circular DNA
Cp	core protein
Cp149	N-terminal domain of the Cp
Cp150	mutant Cp149
CTD	C-terminal domain of the Cp
DBT	dibenzo-thiazepin-2-one
EC_{50}	half maximal effective concentration in cellular assay
EM	electron microscopy
FBS	fetal bovine serum
GPA	glyoxamide-pyrrolamide
HAP	heteroarylpyrimidine
HBcAg	HBV core antigen
HBsAg	HBV surface antigen
HBV	hepatitis B virus
HRP	horse radish peroxidase
IC_{50}	half maximal inhibitory concentration in biochemical assay
NAGE	native agarose gel electrophoresis
PBS	phosphate buffered saline
PPA	phenylpropenamide
PT	pyrazolyl-thiazole
qPCR	quantitative polymerase chain reaction
rcDNA	relaxed circular DNA
SBA	sulfamoylbenzamide

monomer (Wynne et al., 1999). Due to the key role of the Cp at multiple stages in the viral life cycle (Zlotnick et al., 2015; Zoulim, 2005), it is postulated that capsid assembly modifiers (CAMs) may inhibit HBV replication and combat persistence on at least four different levels. Firstly, CAMs may misdirect capsid assembly due to altered assembly kinetics, thereby preventing production of infectious virions (Stray et al., 2005). Secondly, the absence of properly assembled capsids and encapsulated rcDNA genomes blocks the so-called recycling pathway and interferes with the maintenance of the cccDNA pool. Thirdly, CAMs may deplete the pool of free Cp that maintains the cccDNA in a transcriptionally active state (Levrero et al., 2009). Lastly, depletion of the free Cp might remove the block on transcription of interferons and interferon-stimulated genes, leading to restoration of the host's innate immune response (Gruffaz et al., 2013).

CAMs fall into two functional classes: class I CAMs, including the sulfamoylbenzamides (SBAs) and phenylpropenamides (PPAs), induce assembly of morphologically intact, but empty, capsids (Berke et al., 2017; Zhou et al., 2017), while class II CAMs, including the heteroarylpyrimidines (HAPs), provoke the formation of aberrant high-order structures (Berke et al., 2017; Liu et al., 2017; Zhou et al., 2017). In recent years, several new chemical scaffolds showing CAM activity have been identified using screening or rational design (Hartman and Kuduk, 2016; Mani et al., 2018; Turner et al., 2015; Vandyck et al., 2015; Wang et al., 2015; Yang et al., 2016). Of those CAMs which have been classified to date, only HAP belongs to class II. In this study, we analyzed three previously unclassified CAMs belonging to the chemical classes of pyrazolyl-thiazole (PT), glyoxamide-pyrrolamide (GPA) and dibenzo-thiazepin-2-one (DPT) (Fig. 1). To elucidate their modes of action, the novel CAMs were tested in different biochemical and cell-based assays together with a representative each of the HAP, SBA and PPA scaffolds. To our knowledge, this is the first systematic comprehensive assessment in which representatives of six different chemical scaffolds of HBV-specific CAMs have been compared head-to-head in the same assays.

2. Materials and methods

2.1. Compounds

The reference nucleoside inhibitor, entecavir (ETV), was purchased from Selleck Chemicals (Munich, Germany). CAMs shown in Fig. 1 were synthesized as described by Hartman and Flores (2013), Hartman and Kuduk (2016), Perni et al. (2000), Turner et al. (2015), Vandyck et al. (2015). The HAP compound tested, BAY 41–4109, was synthesized at Bayer AG (Wuppertal, Germany) (Deres et al., 2003). All compounds have at least 99% purity.

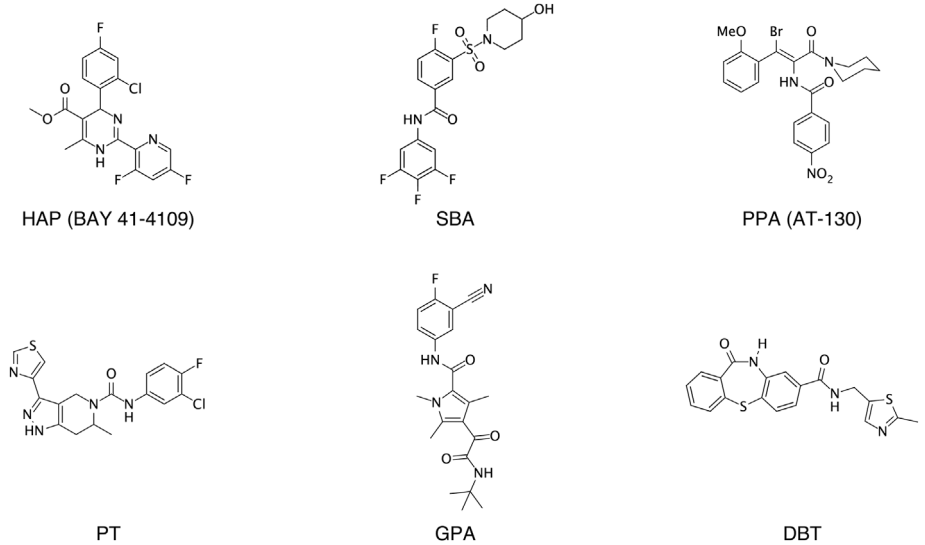

Fig. 1. Chemical structures of the different capsid assembly modifiers used (from top left to bottom right): heteroarylpyrimidine (HAP), sulfamoylbenzamide (SBA), phenylpropenamide (PPA), pyrazolyl-thiazole (PT), glyoxamide-pyrrolamide (GPA), and dibenzo-thiazepin-2-one (DBT).

Table 1
Anti-HBV activity and cytotoxicity of six different CAMs and ETV tested in HepAD38 cells.

Compounds	μm EC_{50} (mean ± SD)	μm CC_{50} (mean ± SD)
HAP	0.068 ± 0.029	> 32
SBA	0.22 ± 0.095	18 ± 3.4
PPA	0.20 ± 0.33	> 32
GPA	0.0014 ± 0.00089	> 100
PT	0.020 ± 0.0099	> 32
DBT	0.14 ± 0.076	> 32
ETV	0.00057 ± 0.00050	> 0.18

*All compounds were tested at least thrice.

2.2. HBV Cp purification

The recombinant Cp assembly domain used in this study has an additional C-terminal cysteine and has all its native cysteines replaced with alanine (Cp150) (Zlotnick et al., 2007). Cp150 was expressed in *Escherichia coli* Rosetta2 (DE3). After extraction using the Qproteome Bacterial Protein Prep Kit (Qiagen) the proteins were precipitated with ammonium sulfate to 40% saturation, and dissolved in Buffer A (100 mM Tris, pH 7.5, 100 mM NaCl, 2 mM DTT). The assembled capsid material was purified using a CaptoCore 700 HiTrap affinity column (GE Healthcare) equilibrated with Buffer A and mounted on an ÄKTA Explorer 10 (GE Healthcare). The resulting flow through was then dialyzed into Buffer N (50 mM sodium bicarbonate, 5 mM DTT, pH 9.6). The capsids were then disassembled into dimers using 3 M urea, and isolated using a Sephacryl S-300 HR XK 50/60 size exclusion column (GE Healthcare) equilibrated with Buffer N. The dimer peak was enriched using an Amicon Stirred Ultrafiltration Cell (Millipore), and dialyzed into HEPES buffer (50 mM HEPES, pH 7.5, 5 mM DTT). To confirm the assembly activity of the isolated dimers, a second round of assembly with 0.5 M NaCl and disassembly with 3 M urea was performed. Assembled capsids and assembly-active dimers were isolated using the same affinity and size exclusion columns, respectively.

2.3. Biochemical capsid assembly assay (CAA)

The assay was performed according to Zlotnick et al. (2007), with some modifications. Briefly, Cp150 was fluorescently labelled at its C-terminus with BODIPY-FL (maleimide) dye (Molecular Probes). Then, 1.5 μM of the labelled Cp150 was incubated for 6 min with various concentrations of test compound in a reaction buffer containing 50 mM HEPES, pH 7.5, 150 mM NaCl and 1% DMSO. Fluorescence was measured on a ClarioStar plate reader (BMG Labtech). In the dimeric state, the fluorescence signal from the dye is high; this is then quenched upon capsid assembly. Assembly was quantified as in Equation (1), where the negative control contains only protein in 50 mM HEPES, pH 7.5.

$$\%\ Assembly = \frac{Sample_{RFU} - Negative\ control_{RFU}}{Negative\ control_{RFU}} \times 100\% \quad (1)$$

2.4. Analytical size exclusion chromatography (aSEC)

Five micromolar Cp150 was incubated in 60 mM BES, pH 6.8, 150 mM NaCl and 1% DMSO and with various concentrations of test compound at 25 °C for 2 h. Afterwards, samples were separated on a Superose6 Increase 10/300 size-exclusion column (GE Healthcare) mounted on an ÄKTA Explorer 10 using the same buffer. The effect of the compound on capsid assembly was derived as the ratio of the area under the curve (AUC) of the capsid peak to the AUC of the dimer peak.

2.5. Electron microscopy (EM)

Samples were incubated as described in Section 2.4, but with test compounds at 50-fold IC_{50} concentration. The assembly products were analyzed at the Electron Microscopy Core Facility in Heidelberg. Samples were adsorbed onto 300-mesh carbon-coated and glow-discharged grids, negatively stained with 3% uranyl acetate in water, and viewed under a transmission electron microscope (Jeol JEM-1400) at 80kV. Images were taken using a TEMCAM F416 camera (TVIPS) and analyzed with ImageJ (National Institutes of Health, ver. 1.51j8).

Table 2
Biochemical target activity of six different CAMs tested on Cp150 *in vitro*.

Compounds	CAA	aSEC
	μm IC_{50} (mean ± SD)	μm IC_{50} (mean ± SD)
HAP	0.34 ± 0.17	0.9 ± 0.1
SBA	1.2 ± 0.45	1.2 ± 0.2
PPA	0.61 ± 0.23	1.3 ± 0.2
GPA	0.60 ± 0.099	1.3 ± 0.4
PT	1.4 ± 0.46	1.5 ± 0.1
DBT	0.70 ± 0.27	1.4 ± 0.2

*CAA = capsid assembly assay, aSEC = analytical size exclusion chromatography, HAP = heteroarylpyrimidine, SBA = sulfamoylbenzamide, PPA = phenylpropenamide, GPA = glyoxamide-pyrrolamide, PT = pyrazolyl-thiazole, DBT = dibenzo-thiazepin-2-one.

2.6. HBV antiviral assay

The HepAD38 cell line, a tetracycline-inducible HepG2 cell line stably transfected with HBV (Ladner et al., 1997), was obtained from Prof. Christoph Seeger (Fox Chase Cancer Center, Philadelphia, PA). In 96-well plates, 80,000 HepAD38 cells/well were seeded without tetracycline, and treated with serial half-log dilutions of test compounds for 6 days. Cell culture supernatants were collected at the end, and HBV DNA was extracted using the MagNAPure Viral Nucleic Acid Universal Small Volume kit (Roche). DNA was then measured using quantitative PCR (qPCR) with HBx-specific primers and probes, and the LightCycler 480 Probes Master kit (Roche). Additionally, identically treated non-HBV expressing HepAD38 cells (i.e., cultured with tetracycline) were used to determine the cytotoxicity of the test compounds. For this, PrestoBlue (Invitrogen) was added on day 6 and the half maximal cytotoxic concentration (CC_{50}) was determined according to the manufacturer's protocol.

2.7. HBV particle gel assay

Intracellular HBV particles were assayed as described by Campagna et al. (2013) and Guo et al. (2006), with some modifications. Briefly, 6-well plates were seeded with 1×10^6 HepAD38 cells/well without tetracycline, and treated with test compounds at 10-fold the half maximal effective concentration (EC_{50}) for 6 days. At the end of treatment, cells were lysed with a buffer containing 10 mM Tris, pH 7.5, 100 mM NaCl, 1 mM EDTA, 0.1% NP-40. Cell debris was pelleted at 5000 g for 10 min. The resulting supernatants were separated on a 4–12% NuPAGE Bis-Tris gel (Invitrogen), and a 1% native agarose gel. The samples were then transferred onto nitrocellulose membranes, and probed with antibodies against HBV core antigen (HBcAg) (Dako B0586) and β-actin (Sigma A1978). Bound antibodies were detected with horse radish peroxidase (HRP)-conjugated antibodies against rabbit (Abcam ab6721) or mouse (Abcam ab6789), and visualized with ECL Prime Western Blotting detection reagent (GE Healthcare).

2.8. Immunofluorescence assay

Sterile cover slips in 6-well plates were seeded at a density of 1×10^5 HepAD38 cells/well. Cells were cultured without tetracycline for 6 days with 10-fold EC_{50} of test compounds. The cells were fixed

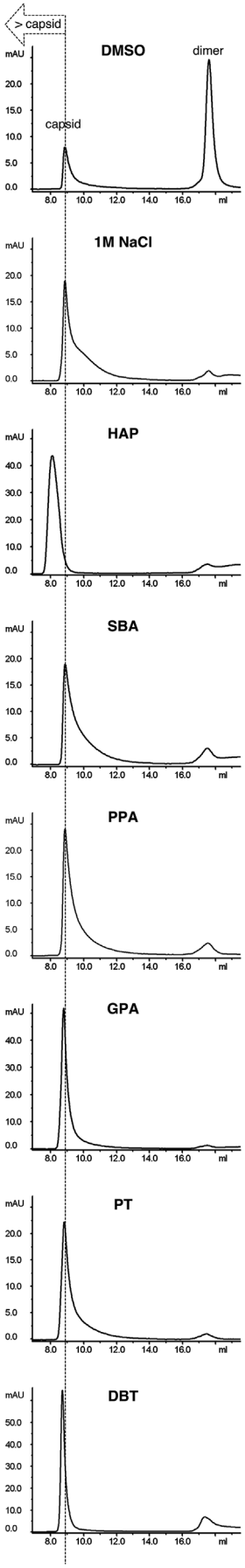

Fig. 2. Analytical size exclusion chromatography of six different CAMs *in vitro*. Cp150 was incubated with 150 mM NaCl and 10 µM compound at 25 °C for 2 h prior to separation on a Superose6 Increase column. Two distinct peaks were observed, with the capsid peak (at ~ 9 mL) eluting before the dimer peak (at ~ 18 mL). The samples incubated with the SBA and PPA compounds showed no shift in capsid peak, while those incubated with GPA, PT, and DBT compounds showed a slight shift. The sample incubated with the HAP compound showed the greatest shift of the capsid peak towards larger structures.

with 4% paraformaldehyde in phosphate buffered saline (PBS), and permeabilized with 0.2% Triton X-100 in PBS. The cells were then blocked with 5% fetal bovine serum in PBS (FBS/PBS). HBcAg was detected with anti-HBc (Abcam ab115992) and anti-rabbit-Alexa 488 antibodies (Invitrogen A-11034) in 5% FBS/PBS. The samples were then mounted using the VECTASHIELD hardset antifade medium with DAPI (Vector Laboratories), and viewed under an inverted fluorescence microscope (Leitz DMRB). Images were taken with the SpotFlex camera and SpotAdvanced 4.6 software (Visitron Systems). Selected samples were also examined using a point-scanning confocal microscope (Leica SP8) with ~0.3 µm optical sections. Images were analyzed using ImageJ (National Institutes of Health, ver. 1.51j8) or Fiji (ver. 2.0.0-rc-65/1.52a).

2.9. Subcellular fraction analysis

Cells were cultured and treated in the same manner as in Section 2.7. Afterwards, cells were washed with PBS and collected from the plate via trypsinization. The cell pellet was then lysed using a hypotonic buffer (10 mM Tris, pH 7.5, 10 mM KCl, 0.1 mM EDTA, 1 mM DTT, cOmplete EDTA-free protease cocktail (Roche), 0.5% NP-40). Samples were briefly vortexed, and the cytoplasmic fraction was separated at 12,000 g for 10 min. The nuclear pellet was then washed three times with the hypotonic buffer without NP-40. Afterwards, the pellet was then resuspended in nuclear extraction buffer (20 mM Tris, pH 7.5, 400 mM NaCl, 1 mM EDTA, 1 mM DTT, cOmplete EDTA-free protease cocktail, 25% glycerol) with periodic mixing. Samples were briefly vortexed, and the nuclear fraction was isolated at 12,000 g for 15 min. The nuclear and cytoplasmic fractions were run on a 4–12% NuPAGE Bis-Tris gel, and transferred onto nitrocellulose membranes. Membranes were probed with antibodies against HBcAg (Dako B0586), α-tubulin (Abcam ab4074) and lamin B1 (Abcam ab16048), followed by a secondary anti-rabbit HRP antibody (Abcam ab6721). Bound antibodies were visualized with ECL Prime Western Blotting detection reagent.

2.10. IC_{50} and EC_{50} calculations

The half maximal inhibitory concentration (IC_{50}) values for the biochemical assays and EC_{50} values for the cell-based assays were calculated from dose-response curves using non-linear regression analysis of GraphPad Prism (GraphPad, ver. 6.03).

3. Results and discussion

3.1. Antiviral activity of different CAMs in HepAD38 cells

The antiviral activities of the six different CAMs were analyzed with the inducible, stably transfected HBV cell line HepAD38. After six days of HBV induction (without tetracycline) in the presence of different concentrations of each CAM, extracellular DNA from cell supernatants was quantified using qPCR. Cytotoxicity of the test compounds was also determined after the same incubation period using the same cell line in the presence of tetracycline to suppress HBV replication. The resulting cell viability was quantified with PrestoBlue. As expected for CAMs, all six different compounds analyzed in this study inhibited HBV DNA replication in a dose-dependent manner, with the most active, the GPA

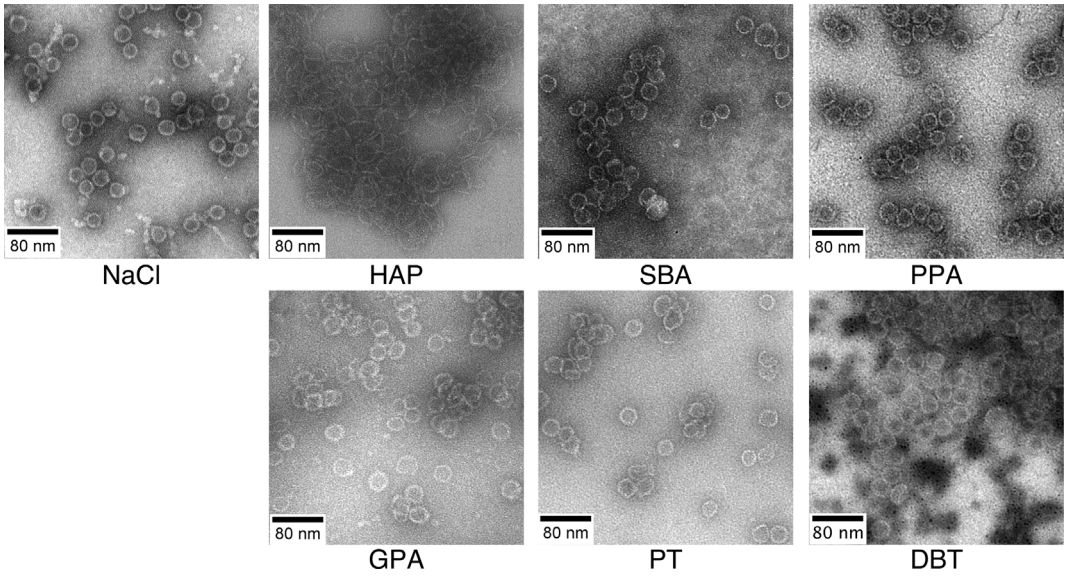

Fig. 3. Electron microscopy analysis of core protein treated with six different CAMs *in vitro*. Cp150 was incubated with 150 mM NaCl and 50-fold aSEC IC_{50} of the compound specified on the bottom of each panel for 1 h at room temperature prior to negative staining. In addition, a positive control of Cp150 incubated with 1 M NaCl was prepared as a reference for normal capsid morphology (upper left). The HAP-treated sample exhibited a distinct morphology with larger structures that tended to aggregate. Cp150 treated with the other CAMs produced morphologically intact capsids.

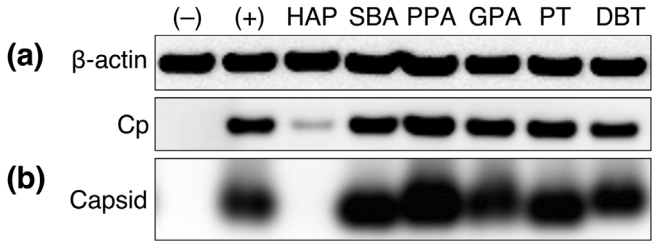

Fig. 4. Intracellular capsid and core protein in HepAD38 cells treated with different CAMs. Cells were cultured with 10-fold the EC_{50} of the respective test compound for 6 days. Proteins in cell lysates were separated by SDS-PAGE (a) and a native agarose gel (b). The negative control (−) shown is lysate from DMSO-treated HepAD38 cells cultured with tetracycline (i.e., with suppressed HBV replication), while the positive control (+) shown is lysate from DMSO-treated HepAD38 cells cultured without tetracycline, allowing HBV replication. Cp and capsids were probed with an anti-HBc antibody (Dako), and β-actin was used as a loading control. Note that in both native and denatured gels the Cp and capsid signal was reduced in HAP-treated cells.

representative with an EC_{50} of 1.4 nM, to the least active, the SBA representative with an EC_{50} of 220 nM (Table 1). In comparison, the positive control ETV showed an EC_{50} of 0.6 nM, in line with published data (Berke et al., 2017). The SBA compound showed the lowest CC_{50} among the CAMs (18 μM), and a selectivity index below 100.

3.2. Effect of different CAMs on HBV capsid formation

By definition, a compound with CAM activity accelerates the HBV capsid assembly reaction in a dose-dependent manner (Stray et al., 2005; Zlotnick et al., 2007). Therefore, we first analyzed the different CAMs in the CAA by monitoring the fluorescence quenching of BODIPY-C-terminally labelled Cp150 in the presence of different CAM concentrations over time. As listed in Table 2, all six CAMs accelerated capsid formation compared to the untreated control with IC_{50} values varying between 0.34 and 1.4 μM. Using this fluorescence quenching assay, HAP showed the highest activity (0.34 μM), whereas SBA and PT showed the lowest activity (1.2 μM and 1.4 μM, respectively).

In an alternative method, we calculated the IC_{50} values from the ratio of the capsid to the dimer peak following aSEC at various CAM concentrations. As shown in Fig. 2, at physiological sodium chloride concentration, the unlabelled Cp150 protein mainly eluted at high retention volume of more than 16 mL, which corresponds to the Cp dimer, whereas at a high sodium chloride concentration of 1 M, the Cp eluted at a lower retention volume (mainly below 12 mL), which corresponds to the high molecular weight capsid. IC_{50} values calculated from aSEC analysis ranged from 0.9 μM to 1.5 μM (Table 2). These values are more closely grouped than those obtained from the CAA. While IC_{50} values can be influenced by the assay conditions, it is important to note that the signal obtained in the CAA to distinguish between dimer and capsid molecules results from the quenching of the fluorescent dye upon capsid assembly. The apparently superior activity of HAP in this assay may result from to its ability to induce formation of aberrant, high-order structures with potentially greater quenching effects.

Additionally, we looked at the retention volume of the capsid peak to get an overall view of its size. As previously described (Berke et al., 2017), only HAP treatment led to a shift of the corresponding capsid peak to lower retention volumes; no shift was observed for the samples treated with the SBA and PPA, in addition to the novel scaffolds GPA, PT or DBT (Fig. 2). By progressively increasing the concentration of the HAP compound up to a maximum of 50 μM, we were able to shift the capsid peak to even lower retention volumes such that the Superose6 column was no longer able to separate the capsid peak (data not shown). Our aSEC data indicate that only the HAP compound exhibits a class II mode of action, whereas results for the SBA, PPA, GPA, PT and DBT compounds were consistent with class I.

3.3. Effect of different CAMs on the morphology of HBV capsids

To further investigate the effect of different CAMs on the morphology of HBV capsids, we performed EM analyses with Cp150 in presence or absence of the CAMs. Consistent with previous studies (Berke et al., 2017; Zhou et al., 2017), no significant morphological changes of capsid structures were induced by class I SBA and PPA compounds, while aberrant structures, with an increased tendency to aggregate were formed after incubation with the class II HAP compound. In this study, no significant changes were also apparent in capsid morphology in samples treated with GPA or DBT (Fig. 3). However, in PT-treated samples, a minor increase in number of abnormally shaped or sized capsids was apparent. These data were

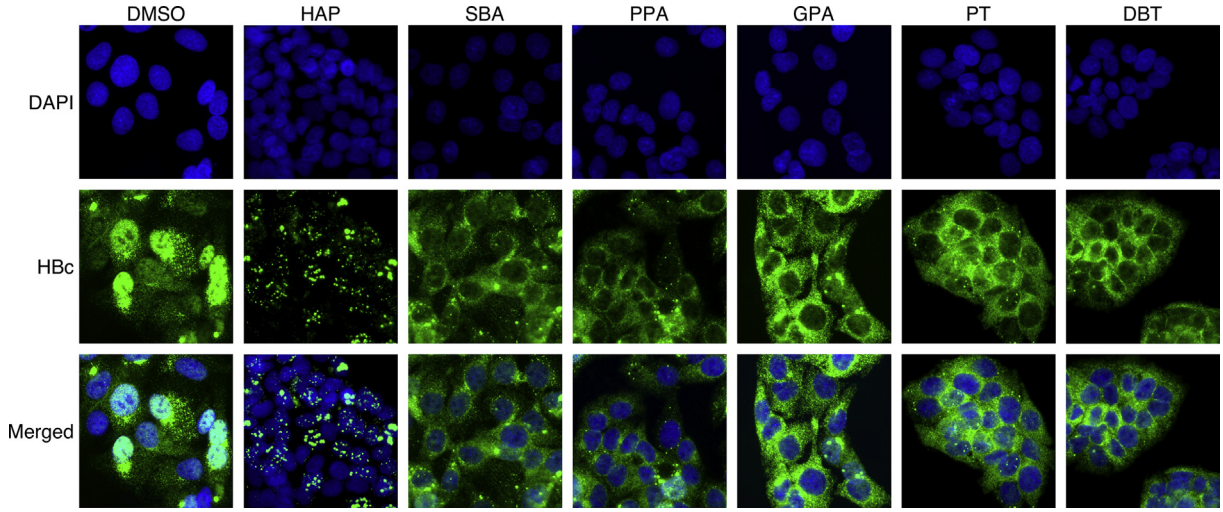

Fig. 5. Immunofluorescence assay of HepAD38 cells treated with different CAMs. Cells were cultured without tetracycline to induce HBV replication and with 10-fold the EC_{50} of the respective test compound for 6 days. HBcAg (green) was visualized via indirect immunofluorescence staining using an inverted fluorescence microscope; nuclear DNA was counterstained with DAPI (blue). The merged images of the two stains are depicted in the bottom row. In DMSO-treated control cells, HBcAg is located in both the nucleus and cytoplasm. In HAP-treated cells Cp displayed punctuated aggregates, while cells treated with all the other CAMs showed almost complete cytoplasmic staining of Cp.

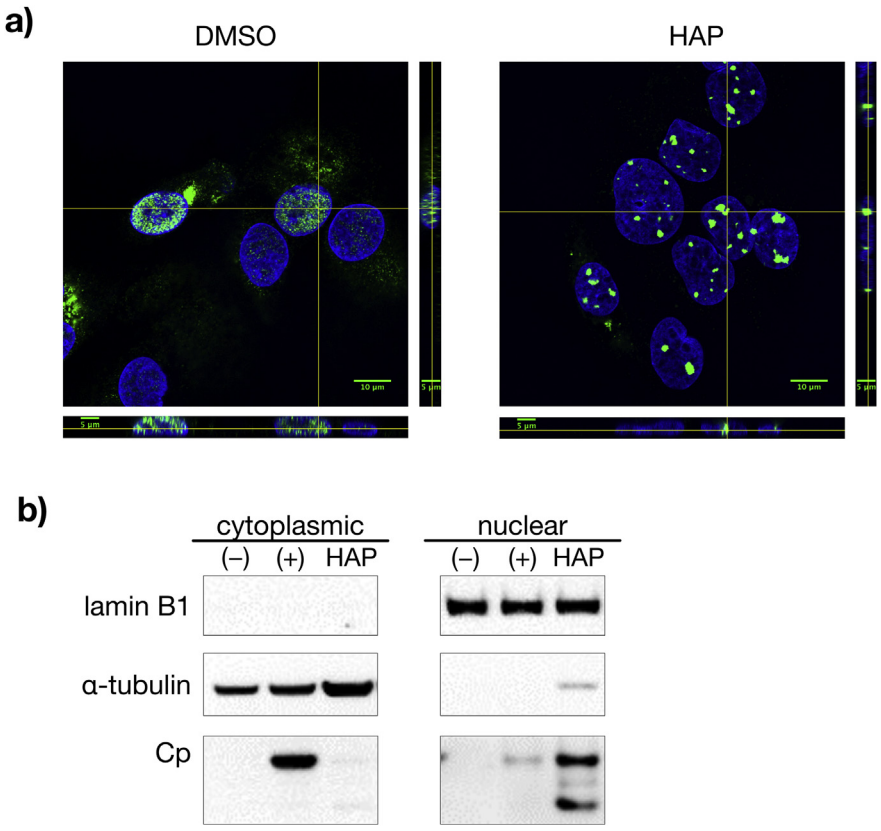

Fig. 6. Subcellular analysis of CAM-treated HepAD38 cells. (a) Immunofluorescence assay samples were viewed with a confocal microscope to visualize nuclear localization of punctate HBcAg (green) aggregates in HAP-treated cells; nuclear DNA was counterstained with DAPI (blue). Representative 3D optical sections (xy and orthogonal views xz and yz) are shown. (b) Cytoplasmic and nuclear fractions of HAP-treated HepAD38 cells were separated using standard fractionation methods and analyzed by Western blot using an anti-HBc antibody (Dako). No Cp was detected in the cytoplasmic fraction of the HAP-treated sample compared to the positive control (+) of DMSO-treated HepAD38 cells cultured without tetracycline. However, for the nuclear fraction, Cp was detected in HAP-treated cells. Lamin B1 and α-tubulin were used as nuclear and cytoplasmic loading controls, respectively. Negative control (−) used was DMSO-treated HepAD38 cells cultured with tetracycline.

consistent with what we observed in the aSEC analysis, wherein HAP-treated samples had the greatest shift in capsid peak retention volume towards larger structures and aggregates (Fig. 2).

3.4. Effect of different CAMs on intracellular core protein concentration and capsid formation in vitro

It has been previously reported that treatment of cells with class I CAM molecules, e.g. the SBA scaffold, does not alter amounts of intracellular Cp and capsid particles, whereas compounds with the HAP scaffold (class II) cause a strong reduction in both intracellular Cp and capsids (Mani et al., 2018; Zhou et al., 2017). To examine the possible differences in the mode of action of the six different CAMs side-by-side, the quantities of intracellular Cp and HBV capsids in compound-treated HepAD38 cells were analyzed using Western blot and particle gel assay. It is important to note that compared to biochemical assays, additional factors come into play in cell culture assays, such as cell permeability, drug solubility, target affinity and binding. The intracellular environment is more complex than that of a simple biochemical assay. In order to reflect the large differences in the antiviral activities of the different

CAM scaffold representatives (Table 1), multiples of EC_{50} rather than equal absolute concentrations were used in the following *in vitro* cell culture assays. As shown in Fig. 4, treatment of the cells with SBA, GPA, PT or DBT compounds at 10-fold EC_{50} did not alter the amounts of intracellular Cp or capsids, as compared to the DMSO-treated control, while PPA showed slightly elevated levels of capsid protein. In contrast, the HAP compound caused a strong reduction in both intracellular Cp and capsid formation (Fig. 4). A study by Deres et al. (2003) has shown that this reduction is mediated by proteasome degradation. Based on this comparison of the intracellular amounts of Cp and capsid particles, we could confirm the hypothesis that all non-HAP CAMs tested in this study share a class I mode of action.

3.5. Effect of different CAMs on the subcellular localization of the HBV core antigen

We used immunofluorescence microscopy to investigate the effects of CAM treatment on intracellular Cp and capsid particle localization. As shown in Fig. 5, after six days of culture, the signal for HBcAg in DMSO-treated control cells could be found distributed throughout the cell and both in the cytoplasm and the nucleus. Interestingly, all non-HAP CAMs induced a completely different phenotype. In SBA, PPA, GPA, PT or DBT compound-treated samples, the signal for HBcAg in HepAD38 cells was located exclusively in the cytoplasm with virtually no apparent nuclear staining. In addition, the amount of cytoplasmic HBcAg seemed to be increased in cells incubated with these CAMs compared to the DMSO-treated control cells (Fig. 5). On the other hand, HAP-treated cells showed punctate Cp aggregates, which under confocal microscopy were observed within the nucleus (Fig. 6a). To further confirm this subcellular localization, cytoplasmic and nuclear fractions of the lysate of HAP-treated cells were analyzed using Western blot (Fig. 6b). Strong reduction of the Cp was observed in the cytoplasmic fraction of the HAP-treated sample. However, in the nuclear fraction, Cp was detected in the HAP-treated sample. In addition to the expected full length Cp band, two lower bands, possibly degraded or truncated Cp products, were observed.

4. Conclusion

The HBV Cp and its assembly into capsids have no known human homologs, making Cp an attractive antiviral target. In addition, due to their alternative modes of action, CAMs are also active against nucleoside/nucleotide analog-resistant mutants (Billioud et al., 2011). Currently, there are several CAMs under clinical development. Studies have shown that although class I and class II CAMs bind to the same pocket on the dimer-dimer interface of the protein, there are differences in the effect exerted on the overall capsid structure, leading to either intact (class I CAMs) or aberrant structures (class II CAMs) (Venkatakrishnan et al., 2016; Zhou et al., 2017). Katen et al. (2013) have proposed that the ability of PPA compounds to induce formation of morphologically intact capsids is due to changes in the tertiary structure of the Cp dimer that permit compensatory changes in the quaternary structure while HAPs do not permit such changes.

The intention of this study was to look at three, so far unclassified, CAM scaffolds, the GPA, PT, and DBT, and compare these head-to-head with the well-characterized SBA and PPA scaffolds as models for the class I mode of action, and HAP scaffold for the class II. Our results suggest that along with the SBA and PPA scaffolds, GPA, PT and DBT scaffolds also exhibit class I modes of action, while the HAP scaffold remains the only identified representative of the class II to date. In addition, we could demonstrate that aside from inducing the assembly of morphologically intact, but empty capsids, class I CAM molecules induce an exclusive cytoplasmic accumulation of Cp. We hypothesize that this could cause a Cp depletion in the nucleus, which might affect some other steps of the viral life cycle such as maintenance of active cccDNA transcription since Cp binding to the minichromosome may alter nucleosome spacing (Bock et al., 2001), and in particular, affect histone acetylation and DNA methylation by interacting with CpG island 2 on the minichromosome (Guo et al., 2011). Another study has shown that Cp in the nucleus may inhibit dsRNA-mediated interferon response either by directly binding to the promoter regions of interferon stimulated genes or recruitment of epigenome-modifying enzymes (Gruffaz et al., 2013).

Interestingly, we found that HAP compound treatment, on the other hand, induced an aggregation of Cp in the nuclei of HBV-producing cells. Very recently, Huber et al. (2018) have shown that these HAP-induced nuclear Cp aggregates are associated with promyelocytic leukemia nuclear bodies, which may lead to different pleiotropic effects such as induction of apoptosis or cellular senescence, which would not be the case with class I CAMs. Further studies are needed to determine whether these differences may impact the potential for CAMs to achieve HBV cure in the clinic.

Declaration of interest

A.C., K.S., A.B., and A.U. are employees of AiCuris Anti-infective Cures GmbH.

Acknowledgments

The authors gratefully acknowledge the guidance of Dr. Marina May in the protein purification, and the excellent technical assistance of Wiebke Schultze, Ilva Leckebusch, Uta Haselmann and the Electron Microscopy Core Facility of the Heidelberg University. We also thank Dr. Rob Saunders, biomed context, for his help editing the manuscript. This project was supported by a research grant from the European Union's Horizon 2020 research and innovation program under the Marie Sklodowska-Curie grant agreement No. 642434.

References

Berke, J.M., Dehertogh, P., Vergauwen, K., Van Damme, E., Mostmans, W., Vandyck, K., Pauwels, F., 2017. Capsid assembly modulators have a dual mechanism of action in primary human hepatocytes infected with hepatitis B virus. Antimicrob. Agents Chemother. 61 e00560-00517.

Billioud, G., Pichoud, C., Puerstinger, G., Neyts, J., Zoulim, F., 2011. The main hepatitis B virus (HBV) mutants resistant to nucleoside analogs are susceptible in vitro to non-nucleoside inhibitors of HBV replication. Antivir. Res. 92, 271–276.

Bock, C.T., Schwinn, S., Locarnini, S., Fyfe, J., Manns, M.P., Trautwein, C., Zentgraf, H., 2001. Structural organization of the hepatitis B virus minichromosome. J. Mol. Biol. 307, 183–196.

Campagna, M.R., Liu, F., Mao, R., Mills, C., Cai, D., Guo, F., Zhao, X., Ye, H., Cuconati, A., Guo, H., Chang, J., Xu, X., Block, T.M., Guo, J.T., 2013. Sulfamoylbenzamide derivatives inhibit the assembly of hepatitis B virus nucleocapsids. J. Virol. 87, 6931–6942.

Deres, K., Schroder, C.H., Paessens, A., Goldmann, S., Hacker, H.J., Weber, O., Kramer, T., Niewohner, U., Pleiss, U., Stoltefuss, J., Graef, E., Koletzki, D., Masantschek, R.N., Reimann, A., Jaeger, R., Gross, R., Beckermann, B., Schlemmer, K.H., Haebich, D., Rubsamen-Waigmann, H., 2003. Inhibition of hepatitis B virus replication by drug-induced depletion of nucleocapsids. Science 299, 893–896.

Gruffaz, M., Testoni, B., Luangsay, S., Ait-Goughoulte, M., Petit, M.A., Ma, H., Klumpp, K., Javanbakht, H., Durantel, D., Zoulim, F., 2013. 378 hepatitis B core (hbc) protein is a key and very early negative regulator of the interferon response. J. Hepatol. 58, S155–S156.

Guo, H., Aldrich, C.E., Saputelli, J., Xu, C., Mason, W.S., 2006. The insertion domain of the duck hepatitis B virus core protein plays a role in nucleocapsid assembly. Virology 353, 443–450.

Guo, Y.-H., Li, Y.-N., Zhao, J.-R., Zhang, J., Yan, Z., 2011. HBc binds to the CpG islands of HBV cccDNA and promotes an epigenetic permissive state. Epigenetics 6, 720–726.

Hartman, G.D., Flores, O.A., inventors; Novira Therapeutics, Inc., assignee. Hepatitis B antiviral agents. World patent WO 2013/096744 A1. 2013 June 27.

Hartman, G.D., Kuduk, S., inventors; Novira Therapeutics, Inc., assignee. Derivatives and methods of treating Hepatitis B infections. World patent WO 2016/109689 A2. 2016 July 7.

Huber, A.D., Wolf, J.J., Liu, D., Gres, A.T., Tang, J., Boschert, K.N., Puray-Chavez, M.N., Pineda, D.L., Laughlin, T.G., Coonrod, E.M., Yang, Q., Ji, J., Kirby, K.A., Wang, Z., Sarafianos, S.G., 2018. The heteroaryldihydropyrimidine bay 38-7690 induces hepatitis B virus core protein aggregates associated with promyelocytic leukemia nuclear bodies in infected cells. mSphere 3.

Katen, S.P., Tan, Z., Chirapu, S.R., Finn, M.G., Zlotnick, A., 2013. Assembly-directed antivirals differentially bind quasiequivalent pockets to modify hepatitis B virus

capsid tertiary and quaternary structure. Structure 21, 1406–1416.
Kay, A., Zoulim, F., 2007. Hepatitis B virus genetic variability and evolution. Virus Res. 127, 164–176.
Ladner, S.K., Otto, M.J., Barker, C.S., Zaifert, K., Wang, G.H., Guo, J.T., Seeger, C., King, R.W., 1997. Inducible expression of human hepatitis B virus (HBV) in stably transfected hepatoblastoma cells: a novel system for screening potential inhibitors of HBV replication. Antimicrob. Agents Chemother. 41, 1715–1720.
Levrero, M., Pollicino, T., Petersen, J., Belloni, L., Raimondo, G., Dandri, M., 2009. Control of cccDNA function in hepatitis B virus infection. J. Hepatol. 51, 581–592.
Liu, C., Fan, G., Wang, Z., Chen, H.S., Yin, C.C., 2017. Allosteric conformational changes of human HBV core protein transform its assembly. Sci. Rep. 7, 1404.
Lok, A.S., Zoulim, F., Dusheiko, G., Ghany, M.G., 2017. Hepatitis B cure: from discovery to regulatory approval. Hepatology 66, 1296–1313.
Mani, N., Cole, A.G., Phelps, J.R., Ardzinski, A., Cobarrubias, K.D., Cuconati, A., Dorsey, B.D., Evangelista, E., Fan, K., Guo, F., Guo, H., Guo, J.T., Harasym, T.O., Kadhim, S., Kultgen, S.G., Lee, A.C.H., Li, A.H.L., Long, Q., Majeski, S.A., Mao, R., McClintock, K.D., Reid, S.P., Rijnbrand, R., Snead, N.M., Micolochick Steuer, H.M., Stever, K., Tang, S., Wang, X., Zhao, Q., Sofia, M.J., 2018. Preclinical profile of AB-423, an inhibitor of Hepatitis B virus pgRNA encapsidation. Antimicrob. Agents Chemother. 62 (6).
Perni, R.B., Conway, S.C., Ladner, S.K., Zaifert, K., Otto, M.J., King, R.W., 2000. Phenylpropenamide derivatives as inhibitors of hepatits B virus replication. Bioorg. Med. Chem. Lett 10, 2687–2690.
Stray, S.J., Bourne, C.R., Punna, S., Lewis, W.G., Finn, M.G., Zlotnick, A., 2005. A heteroaryldihydropyrimidine activates and can misdirect hepatitis B virus capsid assembly. Proc. Natl. Acad. Sci. U. S. A. 102, 8138–8143.
Turner, W.W., Arnold, L.D., Maag, H., Zlotnick, A., inventors; Indiana University Research and Technology Corporation; Assembly Biosciences Inc., assignee. Hepatitis B core protein allosteric modulators. World patent WO 2015/138895 A1. 2015 September 17.
Vandyck, K., Kesteleyn, B., Rudolf, Romanie, Pieters, S., Maria, Aloysius, Rombouts, G., Verschueren, W., Gaston, Raboisson, P., Jean-Marie, Bernard, inventors; Janssen R&D Ireland, assignee. Glyoxamide substituted pyrrolamide derivatives and the use thereof as medicaments for the treatment of Hepatitis B. World patent WO 2015/011281 A1. 2015 January 29.
Venkatakrishnan, B., Katen, S.P., Francis, S., Chirapu, S., Finn, M.G., Zlotnick, A., 2016. Hepatitis B virus capsids have diverse structural responses to small-molecule ligands bound to the heteroaryldihydropyrimidine pocket. J. Virol. 90, 3994–4004.
Wang, Y.J., Lu, D., Xu, Y.B., Xing, W.Q., Tong, X.K., Wang, G.F., Feng, C.L., He, P.L., Yang, L., Tang, W., Hu, Y.H., Zuo, J.P., 2015. A novel pyridazinone derivative inhibits hepatitis B virus replication by inducing genome-free capsid formation. Antimicrob. Agents Chemother. 59, 7061–7072.
World Health Organization, 2017. Hepatitis B: Fact Sheet N° 204. at. http://www.who.int/mediacentre/factsheets/fs204/en/, Accessed date: 23 March 2018.
Wynne, S.A., Crowther, R.A., Leslie, A.G.W., 1999. The crystal structure of the human hepatitis B virus capsid. Mol. Cell 3, 771–780.
Yang, L., Wang, Y.J., Chen, H.J., Shi, L.P., Tong, X.K., Zhang, Y.M., Wang, G.F., Wang, W.L., Feng, C.L., He, P.L., Xu, Y.B., Lu, M.J., Tang, W., Nan, F.J., Zuo, J.P., 2016. Effect of a hepatitis B virus inhibitor, NZ-4, on capsid formation. Antivir. Res. 125, 25–33.
Zhou, Z., Hu, T., Zhou, X., Wildum, S., Garcia-Alcalde, F., Xu, Z., Wu, D., Mao, Y., Tian, X., Zhou, Y., Shen, F., Zhang, Z., Tang, G., Najera, I., Yang, G., Shen, H.C., Young, J.A., Qin, N., 2017. Heteroaryldihydropyrimidine (HAP) and sulfamoylbenzamide (SBA) inhibit hepatitis B virus replication by different molecular mechanisms. Sci. Rep. 7, 42374.
Zlotnick, A., Lee, A., Bourne, C.R., Johnson, J.M., Domanico, P.L., Stray, S.J., 2007. In vitro screening for molecules that affect virus capsid assembly (and other protein association reactions). Nat. Protoc. 2, 490–498.
Zlotnick, A., Venkatakrishnan, B., Tan, Z., Lewellyn, E., Turner, W., Francis, S., 2015. Core protein: a pleiotropic keystone in the HBV lifecycle. Antivir. Res. 121, 82–93.
Zoulim, F., 2005. New insight on hepatitis B virus persistence from the study of intrahepatic viral cccDNA. J. Hepatol. 42, 302–308.